

Exchange bias behavior of monodisperse $\text{Fe}_3\text{O}_4/\gamma\text{-Fe}_2\text{O}_3$ core/shell nanoparticles

Yosun Hwang^a, S. Angappane^{a,1}, Jongnam Park^b, Kwangjin An^b, T. Hyeon^b, Je-Geun Park^{c,d,*}

^a Department of Physics, SungKyunKwan University, Suwon 440-746, Republic of Korea

^b National Creative Research Initiative Center for Oxide Nanocrystalline Materials and School of Chemical and Biological Engineering, Seoul National University, Seoul 151-744, Republic of Korea

^c FPRD & Department of Physics and Astronomy, Seoul National University, Seoul 151-747, Republic of Korea

^d Center for Strongly Correlated Materials Research, Seoul National University, Seoul 151-747, Republic of Korea

ARTICLE INFO

Article history:

Received 28 February 2011

Received in revised form

9 September 2011

Accepted 9 November 2011

Available online 18 November 2011

Keywords:

Fe_3O_4 nanoparticles

Exchange bias behavior

Core-shell structure

ABSTRACT

We have carried out systematic studies on well-characterized monodisperse $\text{Fe}_3\text{O}_4/\gamma\text{-Fe}_2\text{O}_3$ core/shell nanoparticles of 2–30 nm having a very narrow size distribution and possessing a uniquely mono-layer of surface $\gamma\text{-Fe}_2\text{O}_3$. This unique core-shell structure, probably having a disordered magnetic surface state, leads us to three key observations of unusual magnetic properties: i) a very large magnetic exchange anisotropy reaching over 7×10^6 erg/cm³ for the smaller particles, ii) exchange bias behavior in the magnetization data of the core/shell $\text{Fe}_3\text{O}_4/\gamma\text{-Fe}_2\text{O}_3$ nanoparticles, and iii) the temperature dependence of the coercive field following an unusual exponential behavior.

© 2011 Elsevier B.V. All rights reserved.

1. Introduction

Over the past years, we have seen an increasingly large amount of works done on magnetic nanoparticles. With their immense potential applications in very diverse fields of science and technology, a growing number of new nanoparticles have been continuously synthesized and studied [1,2]. Magnetic properties of such nanoparticles are often found to show distinctively different behavior from those of their bulk counterparts. For example, ferromagnetic nanoparticles are found to show enhanced magnetization and magnetic anisotropy, which make them useful for various technological and medical applications in addition to being of greater fundamental interest [3,4].

Some of ferromagnetic nanoparticles exhibit an interesting property called exchange bias, i.e. a displacement of hysteresis loops along the magnetic field axis. It was first reported for fine Co particles, and subsequently attributed to exchange interaction at the interface between ferromagnetic (FM) Co core and antiferromagnetic (AFM) CoO shell [5]. Such exchange bias at the FM/AFM

interface is also expected to give rise to an enhanced coercivity [6]. Despite the original discovery, the exchange bias phenomenon has so far been more systematically studied for thin film systems simply because it is easier to prepare FM/AFM combinations in films with a greater control of the interface than practically possible with nanoparticles, at least until recently [7,8]. However, advances made in the field of magnetic nanoparticle synthesis over last few years [9] have prompted renewed interest in nanoparticles in general, and exchange bias systems in particular.

Of further interest, some selective chemical treatments can be easily done on the surface of nanoparticles: e.g., oxidation, nitration, and sulfation, so opening up a new window of opportunities of tailoring the magnetic properties of nanoparticles by chemical methods. Among Fe-related systems, most works have been so far focused on exchange bias behavior in $\gamma\text{-Fe}_2\text{O}_3$ [10], $\gamma\text{-Fe}_2\text{O}_3$ coated Fe nanoparticles [11] and Fe_3O_4 core (ferri)–FeO shell (AFM) systems [12]. However, there has been so far no report of an exchange bias phenomenon in the core/shell $\text{Fe}_3\text{O}_4/\gamma\text{-Fe}_2\text{O}_3$ nanoparticles, in which the surface of Fe_3O_4 nanoparticles has been naturally modified to $\gamma\text{-Fe}_2\text{O}_3$ shell during the chemical synthetic process. That these Fe_3O_4 nanoparticles have unique biocompatibility with human body adds further motivation to the systematic studies of the nanoparticles, making our results reported here of more than just academic interest.

We report here extensive studies on novel magnetic properties of the core/shell $\text{Fe}_3\text{O}_4/\gamma\text{-Fe}_2\text{O}_3$ nanoparticles by using well-

* Corresponding author. Department of Physics and Astronomy, Seoul National University, Seoul 151-747, Republic of Korea. Tel.: +82 2 880 6613; fax: +82 2 884 3002.

E-mail address: jgpark10@snu.ac.kr (J.-G. Park).

¹ Present address: Centre for Soft Matter Research, Jalahalli, Bangalore 560-013, India.

characterized monodisperse samples of 2–30 nm with a very narrow size distribution and having uniquely one mono-layer of γ - Fe_2O_3 . All our samples were prepared by employing two now well-established methods, developed by us to achieve a 1 nm-scale size control of monodisperse Fe_3O_4 nanoparticles [13,14].

2. Materials and methods

Our nanoparticles were examined by several microscopic tools such as powder X-ray diffraction (XRD), X-ray absorption spectroscopy (XAS), high resolution transmission electron microscopy (HRTEM), and X-ray magnetic circular dichroism (XMCD) to reveal their highly crystalline nature. The HRTEM image in Fig. 1 of our 12 nm particles shows clear lattice fringe patterns, indicative of high quality. Using the XAS data, a quantitative estimation was made of the compositions of iron oxide nano crystals in the form of $(\gamma\text{-Fe}_2\text{O}_3)_{1-x}(\text{Fe}_3\text{O}_4)_x$, wherein x varies from 0.2 to 1.0 with increasing sizes, respectively. The XAS data and our HRTEM image such as the one shown in Fig. 1 taken together constitute the experimental evidence of the core/shell structure of high crystal quality realized in our samples. Using the information from the XAS and XMCD measurements [13] about the volume percentage of γ - Fe_2O_3 , we estimated the volume percentage of Fe_3O_4 to

conclude as shown in Fig. 1 (bottom) that the γ - Fe_2O_3 shell structure corresponds roughly to one mono-layer on the surface of Fe_3O_4 nanoparticles over a wide range in size smaller than ~ 15 nm.

3. Results and discussion

For this study, we used a total of 18 samples prepared in two different methods. The samples A of 9 sizes (2, 3, 3.5, 5, 8, 12, 14, 20, and 30 nm) were prepared with a very fine control of size as described in Ref. [13], while the samples B of another 9 sizes (4, 5, 6, 7, 9, 10, 13, 15, and 30 nm) were prepared following a so-called mass production method reported in Ref. [14]. We measured the temperature dependence of DC magnetization using a SQUID magnetometer (MPMS-5XL, Quantum Design, USA) under an applied field of 100 Oe. The $M(H)$ loops of our nanoparticles were measured in the field range of -1 – 1 T at various temperatures from 5 K to T_B at a constant cooling field. We also varied cooling fields from 0 to 5 T for M – H measurements at 10 K. The exchange bias and mean coercivity, defined as $H_E = (H_{RC} + H_{LC})/2$ and $H_C = (H_{RC} - H_{LC})/2$, where $H_{RC}(H_{LC})$ represents right(left)-hand coercive fields in the positive(negative) field direction, have been determined from the measured $M(H)$ loop.

Fig. 2a shows the magnetization curves of our $\text{Fe}_3\text{O}_4/\gamma\text{-Fe}_2\text{O}_3$ core/shell nanoparticles after normalizing the data for the sake of

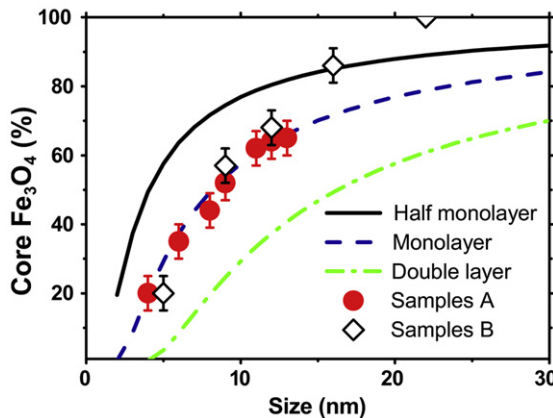
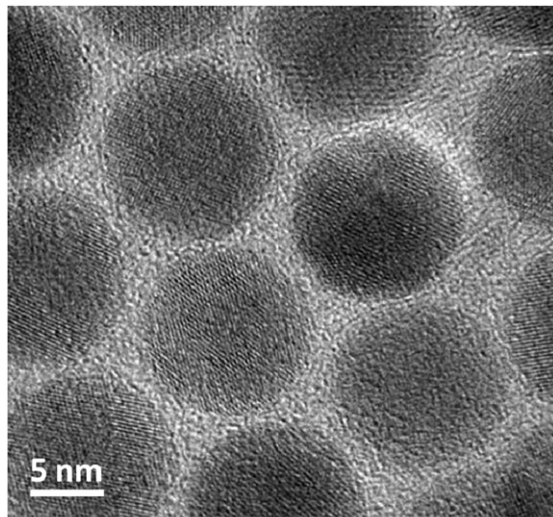


Fig. 1. (Top) HRTEM images of 12 nm $\text{Fe}_3\text{O}_4/\gamma\text{-Fe}_2\text{O}_3$ core/shell nanoparticles. (bottom) Volume percentage of Fe_3O_4 is estimated for samples A and B based on the XMCD data. Lines represent our theoretical estimation of the volume percentage of Fe_3O_4 using different layer thickness of $\gamma\text{-Fe}_2\text{O}_3$.

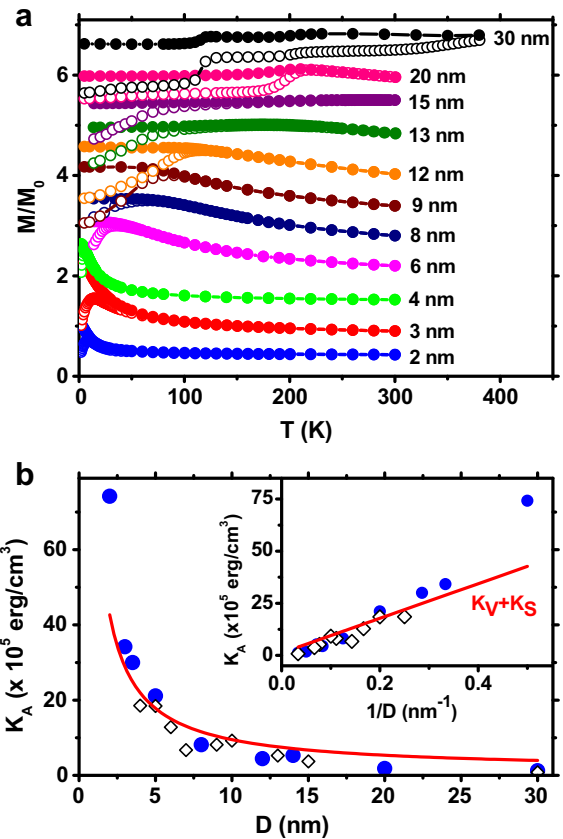


Fig. 2. (a) Normalized M_{ZFC} (open symbols) and M_{FC} (closed symbols) are shown for several $\text{Fe}_3\text{O}_4/\gamma\text{-Fe}_2\text{O}_3$ core/shell nanoparticles with the data shifted upwards for the sake of better presentation. (b) It shows the size dependence of anisotropy constant, K_A of $\text{Fe}_3\text{O}_4/\gamma\text{-Fe}_2\text{O}_3$ core/shell nanoparticles using all the data obtained on the samples prepared in two different methods: the solid symbols are for samples A, while the open symbols are for samples B (see the text). Inset shows K_A vs. $1/D$. Solid lines are fitting result against Eq. (1) with the contributions of volume and surface anisotropies to the anisotropy of $\text{Fe}_3\text{O}_4/\gamma\text{-Fe}_2\text{O}_3$ core/shell nanoparticles.

better presentation. The zero-field-cooled (ZFC) magnetization (M_{ZFC}) of all the nanoparticles shows typical peak features at blocking temperature, T_B , before decreasing thereafter. On the other hand, the field-cooled (FC) magnetization (M_{FC}) exhibits similar behavior to M_{ZFC} above T_B before showing deviations at lower temperatures. Nanoparticles of 30 nm show an additional transition; the Verwey transition of Fe_3O_4 is observed around 120 K, which is absent for all the other samples smaller than 20 nm. It means that the bulk properties of Fe_3O_4 already get recovered in our largest sample of 30 nm, implying that there is a crossover between 20 and 30 nm differentiating the physics of nanoparticles from those of the bulk sample. The blocking temperature increases as expected with increasing particle size. We have calculated the anisotropy constant from the blocking temperature (T_B) using the usual formula: $K_A = 25k_B T_B / V$, where K_A is the magnetic anisotropy energy of a single particle of volume V , k_B is the Boltzmann constant, and T_B is the measured blocking temperature. The size dependence of the anisotropy constant, K_A was determined using the data taken on all our $\text{Fe}_3\text{O}_4/\gamma\text{-Fe}_2\text{O}_3$ core/shell nanoparticles. Our estimate of K_A is 1.2×10^5 erg/cm³ for our biggest nanoparticles with the diameter of 30 nm, which is almost equal to the bulk uniaxial anisotropy constant of Fe_3O_4 [15].

The magnetic anisotropy of our $\text{Fe}_3\text{O}_4/\gamma\text{-Fe}_2\text{O}_3$ core/shell nanoparticles in Fig. 2b increases with decreasing particle size as often found for other nanoparticles possibly due to considerable surface contributions to the magnetic anisotropy [16]. In addition to the usual volume term of the magnetic anisotropy, another term accounting for the surface contribution has been added in order to explain the size dependence of the measured magnetic anisotropy in the following formula:

$$K_A = K_V + \frac{6K_S}{D}, \quad (1)$$

where K_V and K_S are the volume and surface anisotropy energy constants, respectively, and D is the average diameter of the nanoparticles. Fig. 2b (see also the inset) shows the magnetic anisotropy of our $\text{Fe}_3\text{O}_4/\gamma\text{-Fe}_2\text{O}_3$ core/shell nanoparticles together with a theoretical line with Eq. (1). We obtained the following fitting parameters: $K_V = 1.2 \times 10^5$ erg/cm³, $K_S = 0.14$ erg/cm². This value of K_S is comparable to that reported for similar oxide nanoparticles [16,17], leading in our case to a large magnetic anisotropy of over 70×10^5 erg/cm³ for 2 nm nanoparticle, 60 times larger than that of bulk Fe_3O_4 . That there is a certain deviation in the fitting for smaller particles, in particular 2 nm particles, could be due to somewhat more complicated interactions between the core and shell layers because of their comparable size (see also the inset of Fig. 2b).

With the natural core-shell structure of our nanoparticles, we have further investigated the exchange bias behavior in our nanoparticles by cooling the nanoparticles in the presence of magnetic fields and measured $M(H)$ loops at various temperatures. Fig. 3a displays typical hysteresis curves in the representative data, measured at 10 K for 12 nm $\text{Fe}_3\text{O}_4/\gamma\text{-Fe}_2\text{O}_3$ core/shell nanoparticles after zero-field cooling and field cooling under 0.05 and 5 T. As one can see, the shift in the loops towards the negative field direction is clearly seen in the field cooling data demonstrating the exchange bias behavior in our $\text{Fe}_3\text{O}_4/\gamma\text{-Fe}_2\text{O}_3$ core/shell nanoparticles. We obtained the following values of exchange bias: for 0.05 T field cooling $H_E = 140$ Oe; for 5 T field cooling $H_E = 120$ Oe. Similar results were also obtained for other nanoparticles with different sizes. In order to check whether this observation of the exchange bias is due to interparticle interaction or not, we have employed a technique of uniformly dispersing nanoparticles in solution that was developed by us [18]. After dispersing

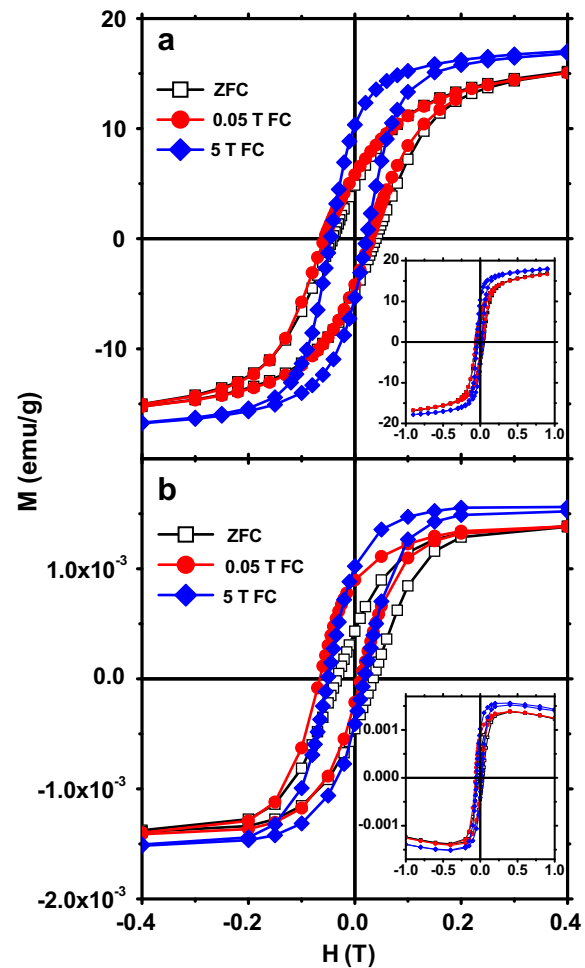


Fig. 3. Hysteresis curves measured at 10 K after zero-field cooling and field cooling under 0.05 and 5 T for 12 nm $\text{Fe}_3\text{O}_4/\gamma\text{-Fe}_2\text{O}_3$ core/shell nanoparticles; (a) powder sample and (b) solution sample. Insets show full hysteresis curves measured up to 1 T.

nanoparticles with interparticle distance larger than 100 nm, i.e. highly diluted solution, we have measured $M(H)$ curves again under the identical conditions. Fig. 3b displays the $M(H)$ curves taken at 10 K on the solution of 12 nm $\text{Fe}_3\text{O}_4/\gamma\text{-Fe}_2\text{O}_3$ core/shell nanoparticles that are dispersed in a mixture of oleic acid and p-xylene. Interestingly enough, the dispersed sample with interparticle distance more than 100 nm still exhibits the exchange bias behavior in much the same way as the powder sample in Fig. 3a: for 0.05 T field cooling $H_E = 270$ Oe; for 5 T field cooling $H_E = 160$ Oe. It is then a clear indication that the observed exchange bias is of an intrinsic single particle property and not related to the interparticle interaction, which is otherwise known to change the magnetic properties of such ferrofluids [19]. Insets of Fig. 3 show that our samples exhibit completely closed loops at 1 T with no visible effects of minor loops. We note that there has been no previous report of the exchange bias behavior for $\text{Fe}_3\text{O}_4/\gamma\text{-Fe}_2\text{O}_3$ core/shell nanoparticles. This natural core-shell structure could in principle favor somewhat strong magnetic interaction between the core and shell parts. For instance, we can think of an interfacial interaction, arising from a somewhat disordered magnetic spins, or sometimes referred to as spin glass state, like $\gamma\text{-Fe}_2\text{O}_3$ coated Fe nanoparticles [7,10,20,21]. In fact, our measurement of one of the samples, 5 nm nanoparticles, shows a clear sign of time dependence, which can be fitted using a stretched exponential function.

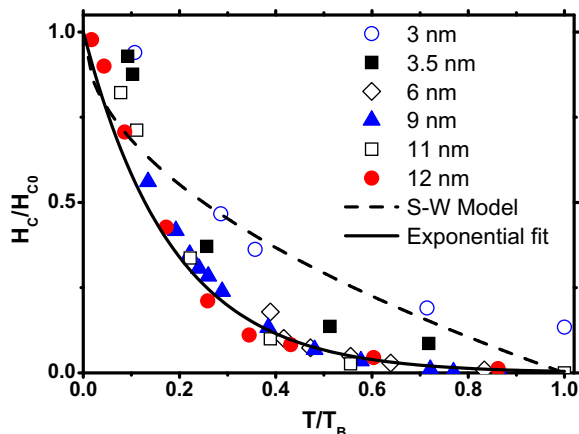


Fig. 4. Normalized coercivity, H_C/H_{C0} is shown as a function of normalized temperature, T/T_B , for all the $\text{Fe}_3\text{O}_4/\gamma\text{-Fe}_2\text{O}_3$ core/shell nanoparticles measured after 100 Oe field cooling. The dashed line represents the usual Stoner–Wolfarth (S–W) model while the solid line is for an exponential dependence.

Fig. 4 shows a gradual increase in the coercivity values of $\text{Fe}_3\text{O}_4/\gamma\text{-Fe}_2\text{O}_3$ nanoparticles with decreasing temperatures below T_B after field cooling with 100 Oe. Because of the magnetic nature of core-shell structure, in particular presumably a disordered magnetic structure of the shell part, our data are not expected to follow the Stoner–Wohlfarth (S–W) model: $H_C(T) = H_{C0}[1 - (T/T_B)^{1/2}]$, for a single domain system as shown by the dashed line in Fig. 4. Instead, we found that the coercivity, $H_C(T)$ can be better fitted to an exponential function, $H_C = H_{C0} \exp(-\alpha T)$. A similar exponential dependence of $H_C(T)$ was observed in amorphous and nanostructured magnetic systems, as well as rare earth transition metal random magnets [21,22]. We note that our two smallest samples show their H_C deviated further from the rest in Fig. 4.

To summarize, we have investigated systematically the magnetic properties of the $\text{Fe}_3\text{O}_4/\gamma\text{-Fe}_2\text{O}_3$ core/shell nanoparticles to find that they exhibit novel exchange bias effects. It is found that the surface anisotropy of large magnitude contributes significantly to the net anisotropy energy of these nanoparticles exceeding $70 \times 10^5 \text{ erg/cm}^3$ for 2 nm nanoparticle, 60 times larger than the bulk value. All our nanoparticles show exchange bias behavior in $M(H)$ curves probably due to the large magnetic anisotropy of the $\gamma\text{-Fe}_2\text{O}_3$ shell with a spin glass-like behavior or a possibly disordered

magnetic state [23]. We have also found an unusual temperature dependence of the coercivity values, following an exponential temperature dependence below T_B .

Acknowledgments

We acknowledge J. H. Park and S. B. Choi for helpful discussion. Works at Seoul National University and SungKyunKwan University were supported by the National Research Foundation of Korea (Grant No. KRF-2008-220-C00012 and R17-2008-033-01000-0). S.A. thanks the Brain Korea 21 program of Korean government for the financial support.

References

- [1] Günter Schmid, Nanoparticles: From Theory to Application. Wiley-VCH Verlag, Weinheim, 2004.
- [2] C.N.R. Rao, P.J. Thomas, G.U. Kulkarni, Nanocrystals: Synthesis, Properties and Applications, Springer Series in Materials Science, vol. 95, Springer, New York, 2007.
- [3] M. Bruchez, M. Moronne, P. Gin, S. Weiss, Science 281 (1998) 2013.
- [4] H. Yan, S.H. Park, G. Finkelstein, J.H. Reif, T.H. LaBean, Science 301 (2003) 1882.
- [5] W.H. Meiklejohn, C.P. Bean, Phys. Rev. 102 (1956) 1413.
- [6] V. Skumryev, S. Stoyanov, Y. Zhang, G. Hadjipanayis, D. Givord, J. Nogués, Nature 423 (2003) 850.
- [7] J. Nogués, J. Sort, V. Langlais, V. Skumryev, S. Suriach, J.S. Muñoz, M.D. Baró, Phys. Rep. 422 (2005) 65.
- [8] Ki-Yeon Kim, Sung-Chul Shin, Yo-Sun Hwang, Younghun Jo, S. Angappane, J.-G. Park, J. Kor. Phys. Soc. 54 (2009) 175.
- [9] D.D. Awschalom, S. Von Molnar, in: G. Timp (Ed.), Nanotechnology, Springer, New York, 1998 Ch. 12.
- [10] B. Martínez, X. Obradors, L. Balcells, A. Rouanet, C. Monty, Phys. Rev. Lett. 80 (1998) 181.
- [11] L. Del Bianco, D. Fiorani, A.M. Testa, E. Bonetti, L. Savini, S. Signoretti, J. Magn. Mater. 262 (2002) 128.
- [12] F.X. Redl, C.T. Black, G.C. Papaefthymiou, R.L. Sandstrom, M. Yin, H. Zeng, C.B. Murray, S.P. O'Brien, J. Am. Chem. Soc. 126 (2004) 14583.
- [13] J. Park, E. Lee, N.-M. Hwang, M. Kang, S.C. Kim, Y. Hwang, J.-G. Park, H.-J. Noh, J.-Y. Kim, J.-H. Park, T. Hyeon, Angew. Chem. Int. Ed. 44 (2005) 2872.
- [14] J. Park, K. An, Y. Hwang, J.-G. Park, H.-J. Noh, J.-Y. Kim, J.-H. Park, N.-M. Hwang, T. Hyeon, Nat. Mater. 3 (2004) 891.
- [15] Z. Kakol, J.M. Honig, Phys. Rev. B 40 (1989) 9090.
- [16] F. Luis, J.M. Torres, L.M. García, J. Bartolomé, J. Stankiewicz, F. Petroff, F. Fetter, J.-L. Maurice, A. Vaurés, Phys. Rev. B 65 (2002) 094409.
- [17] P. Tartaj, T. Gonzalez-Carreno, C.J. Serna, J. Phys. Chem. B 107 (2003) 20.
- [18] C.J. Bae, S. Angappane, J.-G. Park, Youjin Lee, Jinwoo Lee, Kwangjin An, Taegwan Hyeon, Appl. Phys. Lett. 91 (2007) 102502.
- [19] D.A. Dimitrov, G.M. Wysin, Phys. Rev. B 50 (1994) 3077.
- [20] L. Del Bianco, D. Fiorani, A.M. Testa, E. Bonetti, L. Signorini, Phys. Rev. B 70 (2004) 052401.
- [21] R.K. Zheng, G.H. Wen, K.K. Fung, X.X. Zhang, J. Appl. Phys. 95 (2004) 5244.
- [22] J. Tejada, X.X. Zhang, E.M. Chudnovsky, Phys. Rev. B 47 (1993) 14977.
- [23] V. Singh, V. Srinivas, M. Ranot, S. Angappane, J.-G. Park, Phys. Rev. B 82 (2010) 054417.